# INFORMATICS IN SUPER RESOLUTION OPTICAL IMAGING: CHARACTERIZATION OF MITOCHONDRIA IN COCHLEAR HAIR CELLS

By

Rosemary T Nettleton

A CAPSTONE

Presented to The Department of Medical Informatics and Clinical Epidemiology
and the Oregon Health & Science University
School of Medicine
in partial fulfillment of the requirements for the degree of

Master of Biomedical Informatics

December 2013

School of Medicine

Oregon Health & Science University

---

CERTIFICATE OF APPROVAL

This is to certify that the Master's Capstone Project of

Rosemary T. Nettleton

*"Informatics in Super Resolution Imaging: Characterization of Mitochondria in Cochlear Hair Cells"*

Has been approved

Eilis A. Boudreau M.D., PhD.
Capstone Advisor
Department of Medical Informatics and Clinical Epidemiology

# Table of Contents

# List of Illustrations

# Acknowledgements

I first thank my academic advisor, Eilis Boudreau, for her unending support and encouragement. Her inspiration shaped this project and her guidance kept it going even in the darkest hours. To the department of medical informatics and clinical epidemiology, thank you for your support both financially and emotionally. I could not have made it to the end without your willingness to help in any way needed.

Many thanks to Teresa Wilson who provided cell preparation. Your help is deeply appreciated. Hiromichi Yonekawa (Department of animal laboratory science, Tokyo Metropolitan Institute of Medical Science) provided mtGFP-tg transgenic mice. I would also like to acknowledge contributions made by the laboratories of Dr. Alfred Nuttall (Department of Otolaryngology, OHSU) and Dr. Ruikang Wang (Department of Bioengineering, UW). This work was supported by an NIH grant (NIDCD DC 00105).

Finally I thank my children Jeffery, Taylor and Kalii, my mother Meredith and my sister in crime Rhoda for always supporting me no matter what. Through all my years of higher education, you guys have always been there to listen even during my “mad scientist” phase.

# Abstract

Hearing lose affects 360 million people worldwide and a largely preventable contributor is excessive noise. Exposure to loud noise damages the delicate hair cells of the cochlea. The mechanism by which this damage occurs has been linked to overproduction of reactive oxygen species in hair cell mitochondria. Characterization of noise-induced changes in mitochondria has previously been hampered by the lack of microscope technology with adequate resolution. The advent of high-resolution optical imaging techniques has allowed researchers to capture images of cellular structures, such as mitochondria, in intact fixed and live-cells. While imaging techniques have made great strides in the last 20 years, visualization and analysis techniques for super resolution images are lagging behind. Bio-image informatics is an emerging field that aims to employ computational methods to glean additional information from the large image datasets generated by today's high resolution imaging techniques. Available analysis tools are often inaccessible to researchers due to steep learning curves, the need for computer programming experience or the high cost of commercially available software packages. In this capstone project we demonstrate the use of both ImageJ open-source software and commercially available Imaris® software to characterize mitochondria in cochlear hair cells. The application of available image analysis software to today's multidimensional high-resolution imaging data is crucial to understanding the role of mitochondrial changes in noise-induced hearing loss.

# Introduction and Purpose

More than 350 million people worldwide are affected by disabling hearing loss. This includes 32 million children and approximately one-third of the elderly population over 65 years of age [1]. Three principal contributors to acquired hearing loss are age [2], ototoxic drugs [3] and exposure to excessive noise [4]. Nearly half of cases of acquired hearing loss are preventable, especially those caused by loud noise [1]. Noise-induced hearing loss is caused by damage to hair cells of the inner ear [5]. Since these cells do not regenerate, damage results in permanent sensironeural hearing loss. Several lines of evidence suggest that increased levels of reactive oxygen species (ROS) contribute to hair cell damage [6-9] and that mitochondria are involved in ROS production and cell death [5,10,11]. Furthermore, damage to mitochondrial DNA and associated cellular pathways, promotes overproduction of mitochondrial ROS [12] especially under hypoxic conditions [4,13]. However, few studies have evaluated how changes in mitochondrial volume, cell density, cell location and mitochondrial morphology contribute to cochlear hair cell damage and associated hearing loss. There is a critical need for improved techniques for characterizing the mitochondrial changes associated with hair cell damage. Previously, a major barrier to acquiring this knowledge has been a lack of tools with sufficient resolving power to study changes in mitochondrial morphology in response to loud noise. This is changing as super resolution microscopy systems become available.

Super resolution imaging technology, which makes use of advances in microscopic systems, manipulation of fluorescent proteins, and mathematical manipulation of image data, has increased the lateral and axial resolution available to investigators compared to conventional and confocal microscopy. With this level of resolution, scientists now have the ability to examine changes in mitochondria and characterize their role in hair cell degeneration and loss [14,15]. This technology generates large multidimensional datasets that require specialized analysis. In order to realize the full potential of this advanced imaging technology, further work is needed to determine optimal approaches for analyzing this data [16].

Bioimage informatics is an emerging field dedicated to developing the best approaches to enhance the acquisition, distribution, storage and analysis of biological images [17,18]. This capstone project evaluates the feasibility of applying various commonly used informatics algorithms to analyze super resolution images of mitochondria in cochlear hair cells.

# Background

## Historical Perspective

Since the first microscope was created in 1590, and the first living cell was observed nearly a century later, there has been a steady march to increase the microscope's resolving power. Two centuries ago Joseph Jackson Lister showed that several carefully placed weak lenses would reduce image blurring. It was not until nearly 50 years later that Ernst Abbe developed a mathematical model to describe the relationship between resolution and the wavelength of light [19]. This allowed for the calculation of a microscope's maximum resolution. The ultramicroscope, developed in 1903, was the first instrument to image particles smaller than the wavelength of light, overcoming the limitation described by Abbe. The ultramicroscope system was based on light scattering as opposed to reflection and was widely used in the study of colloids. Its illumination method has been extended to the measurement of fluorescence in bioimaging methods today. Another leap in image resolution occurred when the electron microscope was introduced in 1938. This type of microscope does not have the limitation imposed by the wavelength of light since it uses a beam of electrons to create a detailed image of the sample being studied. Electron microscopes still produce the highest resolution images available today. However, electron microscopes are costly and cannot be used to observe live specimens [20]. Additionally, electron microscopy requires extremely thin samples less than 100nm thick. Samples must be thin enough for electrons to pass through them [21]. So, although nanometer scale lateral resolution can be achieved much of the depth

information is lost. Another major disadvantage is that electron microscopy is limited to recording from a single channel, which does not support visualization of differentially labeled cellular components or studies involving co-localization [20]. Conjugation of newly developed fluorescent proteins [22,23] and small organic dyes to cellular organelles such as mitochondria [24], allows for better visualization of cellular components.

In conventional light microscopy the entire sample is illuminated simultaneously. This allows both in-focus and out-of-focus light to contribute to image formation and limits the resolving power. The confocal microscope system increases local contrast by rejecting light that is outside of the focal plain by means of a pinhole (an adjustable confocal aperture). The sample is illuminated point-by-point. To obtain an image of the entire sample, the laser beam is scanned over the specimen. Since the confocal aperture obstructs light from objects outside of the focal plain, confocal imaging greatly improves resolution in the Z direction. This is one of the fundamental advantages of confocal microscopy. Improvements in depth discrimination make it possible to optically slice thick samples, typically up to 100μm. However, little improvement is seen in lateral resolution. Unlike electron microscopy, confocal microscopes take full advantage of fluorescent staining techniques to enhance visualization of differentially stained cellular components and the study of co-localized cellular components in fixed and live cells.

## Imaging Basics

In its most basic form, an image is an array of values or collection of points each with an intensity value relative to a position in a Cartesian coordinate system. Although there are many imaging techniques being used in a number of fields they all have three common features. These include, an energy source, a real world object and a system to interpret and digitize the signal that results from exposure of the object to the energy source. In optical microscopy the energy source is photons (light). The real world object is the sample to be imaged and in most cases the digitizing system consists of a sensor array in a charge-coupled device (a CCD camera) and computers for visualization. Image quality is dependent on the imaging system. One important determinant of image quality is resolution, which is the ability to discern closely located points from each other.

### Image resolution

One simple method for improving image resolution is increasing the number of intensity values that can be encoded. For example, in a binary image there are only two possible values 0 and 1, black or white. The intensity resolution or dynamic range depends on the number of bits available. As the number of bits and gray levels increase so does the ability to discern details in the image. The number of available intensity values is related to the number of bits per pixel. A typical value of 8 bits encodes 256 ($2^8$) shades of gray and 16 bits encodes 65536 ($2^{16}$) grey levels. In color images each pixel is a combination of three scales for example red, blue and green (RGB). However, a simple increase in intensity resolution is not sufficient in images produced by today's

sophisticated optical imaging methods. Imaging of subcellular components requires a high spatial resolution. But the properties of light limit the achievable resolving power of optical microscopes.

The ability of conventional microscopy to resolve two objects is limited by the diffraction barrier, fist noted in the seminal paper of Ernst Abbe in 1873 [19]. The diffraction limit states that the resolving power of a microscope or other optical instrument (camera, telescope) is limited by the wavelength of light according to the following equation:

$$d = \lambda/2[\eta \sin(\alpha)]$$

Where d is the minimum resolvable diameter, $\lambda$ is the wavelength of the illuminating light, $\eta$ is the refraction index of the imaging medium (typically air, or immersion liquid) and $\alpha$ is the half-angle of incidence the light extends to a focal point. This fundamental limitation of optical imagery means that objects smaller than half the wavelength of the light used cannot be resolved. A measure of this limitation is the point spread function (PSF), which defines the spread of diffracted light from a single point source. In the X and Y directions the PSF appears as an airy disc while in the Z direction the PSF is hourglass shaped. The PSF of a particular imaging system determines the amount of image degradation that can be expected.

Super resolution imaging techniques are considered methods that exceed the Abbe limit. Each technique is based on a distinct physical principle that determines its resolving power. There are two major categories of super resolution imaging techniques. First are interferometric techniques, which

improve the PSF of the imaging system. For example structured illumination microscopy uses optical methods to reduce the size of the airy disc. The other category is single molecule localization, which uses photoswitching to isolate fluorophores and precisely locate the center of the PSF of molecules that would otherwise be unresolvable [25]. For instance, in photoactivation localization microscopy (PALM) a subset of fluorescent molecules are selectively activated, localized and deactivated [14]. The process is repeated until the coordinates of all fluorophores are determined. Our discussion will concentrate on structured illumination, from the first category of super resolution imaging.

Structured illumination is a widefield microscopy technique that exceeds Abbe's diffraction limit by superimposing a known interference pattern on the sample during imaging [26]. The interaction between the scattering of light from the sample and the controlled pattern creates interference patterns (moiré fringes) that carry high-resolution sample information. Several images are taken as the superimposed pattern is rotated in a precise manner. The high resolution image is recovered during post processing. Using this imaging technique, Guffstafsson was able to increase image resolution by a factor of two [27]. Taking this concept further, Keller and colleagues devised an imaging method using incoherent as opposed to coherent light [28]. They were able to achieve a five-fold increase in image contrast. Most importantly, the increase was not achieved at the expense of imaging depth, a problem of electron microscopy. The advantage of structured illumination over confocal microscopy is the preservation of sample luminescence. The signal from samples stained with

bioluminescent dyes is often weak. The loss of essential in-focus light along with the rejected out-of-focus light in confocal microscopy may not return an adequate signal. Furthermore, while confocal microscopy greatly improves axial resolution little lateral resolution is gained.

# Methods

## Animal Model

Cochlear hair cells were collected from the transgenic mouse strain mtGFP-tg [29]. This transgenic mouse strain ubiquitously and exclusively expresses Green fluorescent protein (GFP) in the mitochondria. Advantages of mice expressing GFP include: 1) No staining is required consequently, cells can be imaged directly after preparation. The staining process damages cells [29]. In addition, staining processes often result in uneven fluorescence that can produce artifacts 2) An increase in the signal to noise ratio can be achieved since fluorescence of GFP in mtGFP-tg mice showed no diffusion. 3) The mitochondria of mtGFP-tg mice are resistant to photobleaching.

Studies were conducted in accordance with the guidelines adopted by the National Institutes of Health *Guide for the Care and Use of Laboratory Animals* and with the Oregon Health & Science University Institutional Animal Care and Use Committee approval.

## Cell Preparation and Imaging Parameters

Cell preparation has been described in detail elsewhere [30]. Teresa Wilson (Department of Otolaryngology, OHSU) conducted cell preparation. Vibratome tissue sections were 60μm thick and fixed in 4% paraformaldehyde/0.25% glutaraldehyde. Sections were mounted on slides with CFM-1 PLUS mountant solution from EMS. Cells were imaged using the Ziess LSM710 microscope using structured illumination microscopy (SIM) available in

the Oregon Health and Science University Advanced Light Microscopy Core. The images were collected in a Z-stack containing 130 images and 65 to 72 slices. Total image size is 970 X 970 X 65 pixels in XYZ directions with 16 bits per pixel and a voxel size of 0.04μm in X and Y and 0.14μm in the Z direction.

## Image Processing and Analysis

Multiple steps were required for the full analysis. They included image restoration (deconvolution), image segmentation and 3D image rendering.

Images were analyzed using FIJI (Fiji Is Just ImageJ) [31] with ImageJ[32] version 1.48g (NIH) open source software or Imaris® (Bitplane, version 7.2) commercial software. Deconvolution was performed using Zen2012 software (Ziess).

### Restoration

Image restoration is the process by which image quality is improved using *a priori* knowledge of the imaging system. Optical imaging systems such as microscopes are convolution operators. The measure of how light behaves in a system is the point spread function (PSF). In order to reverse the effects of convolution, mathematical models are constructed that define the amount of blurring for any given microscopy system and based on this a reversing function is applied. Zen software by Zeiss was used to perform deconvolution of SIM images. Zen software uses the algorithms developed by Agard and Sedat [33]. Detailed explanation of this method is beyond the scope of this manuscript. In brief, Agard and Sedat used a constrained iterative process. The PSF is determined based on the blurring of a fluorescent bead. The reversing function is

then applied to each image voxel; the PSF is updated and the function applied again. Constraints on the value of intensities in the image, such as setting artificially generated negative intensities to zero, reduce the contribution of noise to the PSF.

**Segmentation**

Image segmentation is the process of isolating image features. There are many different techniques and algorithms used in image processing. However, due to the complexity of biological images standard segmentation methods may not be adequate.

Thresholding is one of the simplest and widely used segmentation methods. It has been implemented using a variety of algorithms. We applied three thresholding algorithms in an effort to segment mitochondria in our structured illumination images. The Otsu method is an iterative thresholding method that calculates the best threshold value by minimizing the sum of the intensity variance between pixels classified as either foreground or background [34]. The IsoData method is an iterative clustering algorithm. The image histogram is separated into foreground and background using a threshold value equal to half the dynamic range. The average of the two groups is calculated and becomes the subsequent threshold choice. The process is repeated until the threshold value remains stable [35]. The Mean method simply uses the mean of the image grey levels as the threshold. Many algorithms use the Mean method as an initial threshold estimate. The auto threshold feature of ImageJ provides a

way to view the image threshold result of each of these methods and several other methods as well. This type of comparison was not available in Imaris®.

***Morphological segmentation***

Edge detection methods were used to segment cells and then to further segment mitochondria within the region of interest. We created a maximum image projection (MIP) of the original image stack and transformed the image to an 8bit binary image. In order to create smooth contours we applied a morphological dilation. Finally we used the Sobel edge detector with two 3x3 kernels, to highlight sharp changes in intensity.

**3D rendering**

ImageJ provides a pluggin for 3D rendering of images. However, we found that the commercial software, Imaris®, not only provided a more visually attractive rendering but a highly interactive model. We were able to view mitochondria throughout the cell as we adjusted the threshold. Imaris® uses the marching cube algorithm to create the IsoSurface. In short, sets of specialized cubes are fit to the object 8 pixels at a time. The edges of the object that fit within the contours of the 8 pixels are assigned to the volume of the object while those outside are assigned to background. The review by Newman and Yi gives a detailed description of this algorithm [36]. We used the Surpass 3D display mode of Imaris® to create an IsoSurface model of a cochlear hair cell previously segmented from an image containing several cells. The IsoSurface module steps through several parameters. First we adjusted the threshold to 60 to eliminate weakly fluorescent objects. Then smoothed the image with a Gaussian filter with

a width of 3.0μm and selected the function that closes object borders that may be cut open at the edges of the image (Close object Borders). Using the statistics function we were able to calculate an average mitochondrial volume based on this IsoSurface. Next, in order to count the number of mitochondria in the cell, we used the Imaris Spot module, which places a spot at the intensity center of objects of approximately the specified volume. Although Imaris® provides a region-growing algorithm, we chose to use the local contrast model that gave a more consistent outcome. We started with the original thresholded image and adjusted the dynamic range of the gray levels (spot quality) to eliminate spots with low intensity values. To eliminate small artifacts, we only included IsoSurface objects that were greater the 22 voxels in size. We used the volume obtained from the IsoSurface as the spot seed volume.

# Results

Figure 1 shows the change in image quality after application of the deconvolution algorithm of Agard and Sedat [33]. The image quality is significantly improved with much sharper image objects.

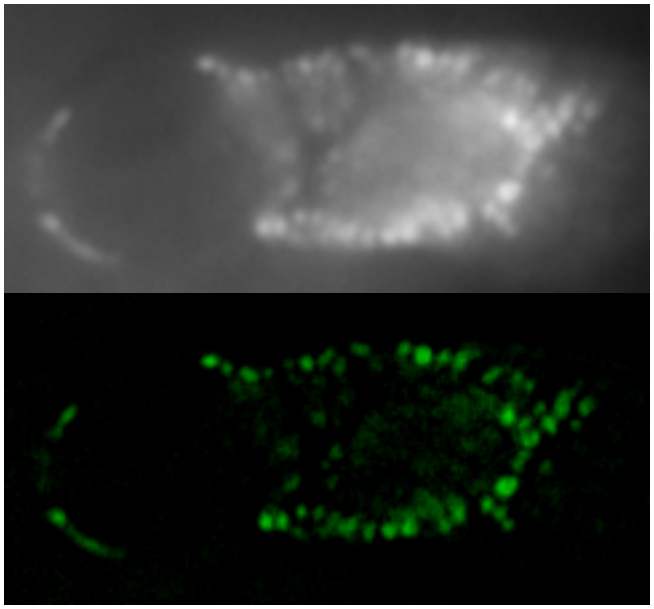

Figure 1 Improvement of image quality after application of deconvolution algorithm. A) Raw image B) Image after deconvolution

We applied three image segmentation algorithms Otsu, IsoData and Mean grey level, available in ImageJ. In figure 2 it can be seen that the choice of algorithm influences the quality of the segmentation. From a visual inspection the Otsu and IsoData algorithms, having arrived at comparable threshold values, give similar results. The Mean algorithm, however, performs poorly in this instance. It gave a significantly lower threshold value, compared to the other algorithms, which did not eliminate sufficient background noise.

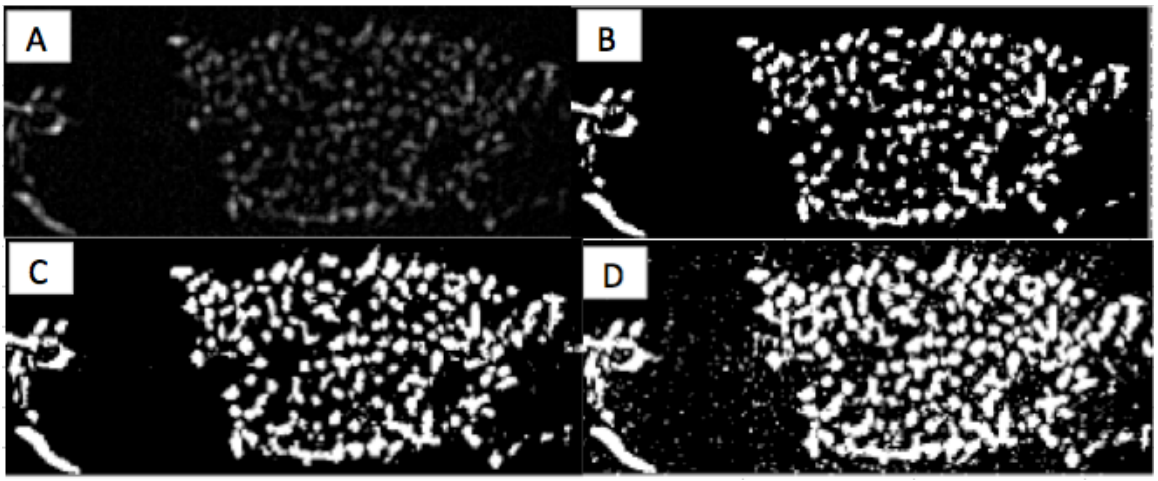


Figure 2 Result of thresholding algorithms. A) Original image B) Otsu C) IsoData D) Mean grey level.

The use of edge detection and morphological operations yielded good results using ImageJ. The result of each step is shown in figure 3. The combination of the Z-projection (figure 3A) and the morphological dilation (figure 3B) produced a sharp contrast that distinguishes the edges of each cell. The edge detector created an outline based on this distinction (figure 3C). For emphasis of the result we also created an overlay on the maximum intensity projection (MIP) image (figure 3D).

The 3D IsoSurface model created with Imaris® software is shown in figure 4A. Although this image shows distinct mitochondria, the creation of the image was labor intensive requiring much manual intervention to adjust parameters specific to this image, and would not be suitable for high-throughput automatic segmentation.

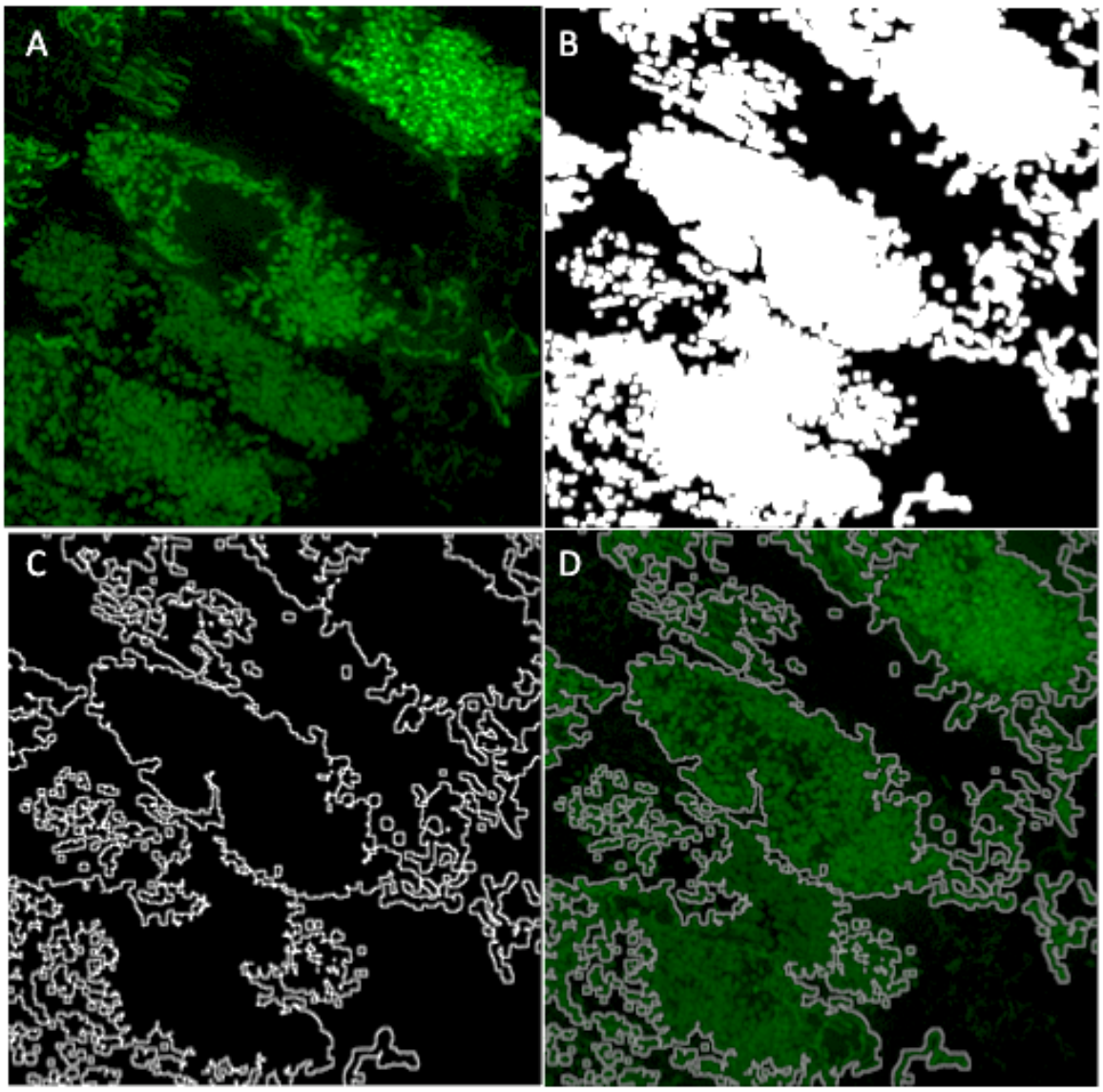


Figure 3 Series of edge detection images created in ImageJ (NIH). A) Maximum intensity projection of the original image stack B) Binary image after morphological dilation to create smooth edges C) Application of the Sobel edge detection algorithm D) Overlay of the edge detection result on the MIP image.

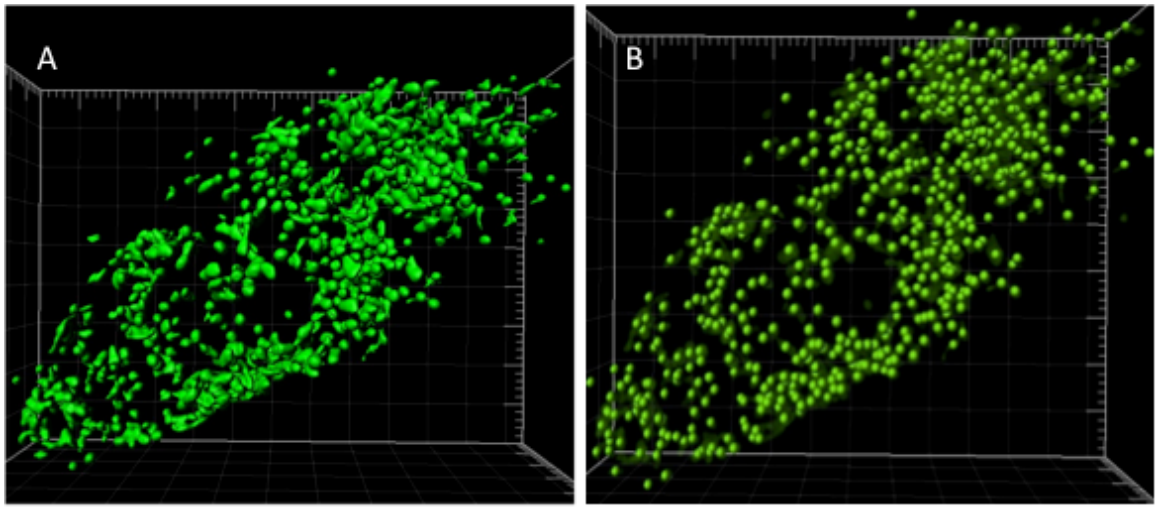


Figure 4 Three-dimensional rendering of mitochondria in a cochlear hair cell. A) Imaris® (Bitplane) IsoSurface model to determine mitochondrial volume B) Result of spot module analysis to obtain a mitochondrial count.

The spot module of Imaris® provided a count of mitochondria. It places a spot on the highest intensity center of each object that is approximately the specified volume. We entered the average volume calculated from the IsoSurface model as the spot seed volume from which Imaris® constructed a 3D image showing the location of individual mitochondria (figure 4B).

# Discussion

Super resolution imaging makes it possible to image cellular organelles such as mitochondria. However, further optimization of approaches to analyze and visualize image datasets is needed to efficiently improve our understanding of subcellular structures. Furthermore, labor-intensive steps should be automated to support high-throughput processing. The project we have described was designed to demonstrate the use of common informatics algorithms in determining the volume and count of mitochondria in cochlear hair cells. The results of this approach will allow researchers to determine how mitochondrial changes contribute to noise-induced hearing loss.

In this analysis we chose the thresholding methods (Otsu and IsoData) that best separated the mitochondria from the image background based on visual inspection. A better method to evaluate algorithm effectiveness was proposed by Otsu in 1973 based on the intensity histogram of gray-level images [34]. Otsu's method is predicated on selection of the algorithm that maximizes the difference criteria between object pixels and background pixels. This method could be adapted to be a measure of algorithm performance. The comparison of an image processing technique to ground truth is currently a problem in analysis of super resolution images. This is mainly because there are few publicly available image datasets for such a validation and in the characterization of mitochondria, to our knowledge, there are no available datasets. Coelho et al 2009 describes manually processed images that can be used as ground truth [37]. They also

discuss methods that can be used to evaluate the performance of segmentation algorithms.

The combination of morphological operations and edge detection techniques provides a clean segmentation of cells. However, edge detection algorithms are computationally expensive. Continued progress in creating more efficient edge detection methods would provide faster analysis of large biological data sets

The rendering of 3D models provides an informative way to display and view 3D datasets. Imaris® provides a step-by-step process to create 3D models that can be viewed from all directions. However, this process is labor intensive and highly subjective. Furthermore, the complex nature of biological images would not allow for automated analysis of several images. With Imaris®, the user has less control over the analysis process than with ImageJ. However, the advantage of Imaris® 3D modeling and visualization is that it gives researchers with expertise in biological systems, but not with computer programming, the ability to use sophisticated image processing techniques. With the IsoSurface model we approximated the volume of mitochondria, however, this value is highly subjective as several manual manipulations of the image were required. We took the average volume obtained from the IsoSurface model as the initial volume in the spot analysis. The 3D spot module uses this volume to place a spot on each object of that approximate size. Although the volume was only an approximation, this method worked well for counting mitochondria as we found that small shifts (2stdv) did not significantly impact the count. This method could also be used to

observe changes in mitochondrial location within the cell in response to loud noise or other noxious stimuli.

In this manuscript, we have demonstrated the use of a few of the most commonly used informatics algorithms in image processing. While these algorithms are widely used in medical image analysis, the added complexity of biological images and the nanoscale nature of the objects of interest require sophisticated techniques and tools.

While imaging technology has made great strides, advances in processing and visualization of the large amount of data generated by super resolution microscopy (SRM), is trailing behind. As SRM becomes a staple of modern research the need for user friendly and readily available post processing software has become critical to realizing the full research potential of images produced in this manner. Fortunately, open source and commercial tools are rapidly being developed.

***Image Processing Tools***

Digital image processing hit its stride in the medical field with analysis approaches that highlight macroscopic features such as tumors. However, application of these processing techniques does not translate to microscopic examination of image features on the nanoscale level. For example, macroscopic bodies in Optical Coherence Tomography (OCT) or Computed Tomography (CT) scans are routinely identified visually with borders manually drawn by a physician. This simple segmentation method is highly impractical for the identification of hundreds of mitochondria in what could potentially be thousands

of images. In developmental biology it is not uncommon to collect a series of images totaling in the thousands and spanning days [28]. Clearly, an imaging project of this magnitude would not be feasible without the availability of efficient image processing tools and automating algorithms.

Open source tools, such as ImageJ, consist of a collection of task-oriented plugins written by members of the scientific community [32]. The advantages of this distribution method are many. The cost is negligible and the software is available to the general public. Furthermore, plugins have already been written to address an array of image processing steps required in the average imaging project. Documentation is readily available; each plugin usually contains a vignette that describes the package and includes examples. Finally, forums can easily be found on the Internet for many disciplines where individual questions can be posed and are answered by either those with a similar experience or experts in the field. On the other hand, there is usually a steep learning curve for the majority of researchers whose main focus is biological mechanisms, not computer programming or image processing. Another disadvantage of the open source paradigm is the dizzying array of available tools. It is often difficult to determine which plugin is best for any given research project. Collections of the most commonly used image processing algorithms have been assembled into suites such as FIJI. Commercially available software while highly documented and generally designed for ease of use, can be cost prohibitive for most laboratory settings and especially for the individual user. More importantly, commercial software can become a “black box” where the user does not have

control or knowledge of the algorithms and parameters used in image processing tasks. Both open-source and commercial software provide compatibility with several of the proprietary file formats used by microscope manufacturers.

Other aspects of imaging projects that have not been discussed in this manuscript but need to be addressed include: image storage and sharing, image registration and standardized image annotation. Storage and sharing of large datasets can be daunting. With researchers generating hundreds of terabytes of imaging data, it becomes necessary to have a devoted server for adequate and safe storage of images. Many imaging projects involve more than one imaging modality and differences in temporal resolution and differences between subjects often require registration of images to one another or to an established image atlas. Finally, there is a great need to standardize image annotation. Image metadata is critical to image sharing and reproducibility of image processing workflows. Annotation of images is a necessary step in the ability to create image databases that would facilitate the advancement of super resolution imaging projects.

In conclusion, imaging techniques have made great strides in the last 20 years. Super resolution microscopy has exceeded the limits of conventional microscopy, giving researchers the ability to capture images of subcellular components, such as mitochondria. The large multidimensional image datasets that this technology generates requires sophisticated analysis methods. We have demonstrated the use of just a few key informatics algorithms in analyzing super resolution images of mitochondria in cochlear hair cells. This approach can also

be used to evaluate other nanoscale components such as cellular nuclei and the cellular cytoskeleton. As imaging takes a pivotal role in modern research, the continued development of image analysis approaches is crucial to advancing our understanding of subcellular structures and their contribution to disease states such as noise-induced hearing loss.

# References


1. WHO factsheets. World Health Organization Web site. www.who.int/mediacentre/factsheets/fs300/en/index.html. Published Feb. 2013. Updated 2013. Accessed November, 2013.

2. Cruickshanks KJ, Tweed TS, Wiley TL, et al. The 5-year incidence and progression of hearing loss: The epidemiology of hearing loss study. *Arch Otolaryngol Head Neck Surg*. 2003;129(10):1041-1046.

3. Barrenas ML. Hair cell loss from acoustic trauma in chloroquine-treated red, black and albino guinea pigs. *Audiology*. 1997;36(4):187-201.

4. Nuttall AL. Sound-induced cochlear ischemia/hypoxia as a mechanism of hearing loss. *Noise Health*. 1999;2(5):17-32.

5. Hu BH, Guo W, Wang PY, Henderson D, Jiang SC. Intense noise-induced apoptosis in hair cells of guinea pig cochleae. *Acta Otolaryngol*. 2000;120(1):19-24.

6. Yamashita D, Jiang HY, Schacht J, Miller JM. Delayed production of free radicals following noise exposure. *Brain Res*. 2004;1019(1-2):201-209.

7. Van Campen LE, Murphy WJ, Franks JR, Mathias PI, Toraason MA. Oxidative DNA damage is associated with intense noise exposure in the rat. *Hear Res*. 2002;164(1-2):29-38.

8. Cassandro E, Sequino L, Mondola P, Attanasio G, Barbara M, Filipo R. Effect of superoxide dismutase and allopurinol on impulse noise-exposed guinea pigs--electrophysiological and biochemical study. *Acta Otolaryngol*. 2003;123(7):802-807.

9. Henderson D, Bielefeld EC, Harris KC, Hu BH. The role of oxidative stress in noise-induced hearing loss. *Ear Hear*. 2006;27(1):1-19.

10. Karbowski M, Youle RJ. Dynamics of mitochondrial morphology in healthy cells and during apoptosis. *Cell Death Differ*. 2003;10(8):870-880.

11. Turrens JF. Mitochondrial formation of reactive oxygen species. *J Physiol*. 2003;552(Pt 2):335-344.

12. yamasoba t. Role of mitochondrial dysfunction and mitochondrial DNA mutations on age-related hearing loss. . 2007.

13. Hoffman DL, Salter JD, Brookes PS. Response of mitochondrial reactive oxygen species generation to steady-state oxygen tension: Implications for hypoxic cell signaling. *Am J Physiol Heart Circ Physiol*. 2007;292(1):H101-8.

14. Brown TA, Fetter RD, Tkachuk AN, Clayton DA. Approaches toward super-resolution fluorescence imaging of mitochondrial proteins using PALM. *Methods*. 2010;51(4):458-463.

15. Shim SH, Xia C, Zhong G, et al. Super-resolution fluorescence imaging of organelles in live cells with photoswitchable membrane probes. *Proc Natl Acad Sci U S A*. 2012;109(35):13978-13983.

16. Zhu L, Zhang W, Elnatan D, Huang B. Faster STORM using compressed sensing. *Nat Methods*. 2012;9(7):721-723.

17. Eliceiri KW, Berthold MR, Goldberg IG, et al. Biological imaging software tools. *Nat Methods*. 2012;9(7):697-710.

18. Peng H. Bioimage informatics: A new area of engineering biology. *Bioinformatics*. 2008;24(17):1827-1836.

19. Abbe E. Beitrage zur theorie des mikroskops und der mikroskopischen. *Archv fur Mikropische Anatomie*. 1873(9):413.

20. Schermelleh L, Heintzmann R, Leonhardt H. A guide to super-resolution fluorescence microscopy. *J Cell Biol*. 2010;190(2):165-175.

21. Mayer J, Giannuzzi L, Kamino T, Michael J. TEM sample preparation and FIB-induced damage. *MRS Bulletin*. 2007;32:401.

22. Heilemann M, van de Linde S, Schuttpelz M, et al. Subdiffraction-resolution fluorescence imaging with conventional fluorescent probes. *Angew Chem Int Ed Engl*. 2008;47(33):6172-6176.

23. Betzig E, Patterson GH, Sougrat R, et al. Imaging intracellular fluorescent proteins at nanometer resolution. *Science*. 2006;313(5793):1642-1645.

24. van de Linde S, Sauer M, Heilemann M. Subdiffraction-resolution fluorescence imaging of proteins in the mitochondrial inner membrane with photoswitchable fluorophores. *J Struct Biol*. 2008;164(3):250-254.

25. Patterson G, Davidson M, Manley S, Lippincott-Schwartz J. Superresolution imaging using single-molecule localization. *Annu Rev Phys Chem*. 2010;61:345-367.

26. Bailey B, Farkas DL, Taylor DL, Lanni F. Enhancement of axial resolution in fluorescence microscopy by standing-wave excitation. *Nature*. 1993;366(6450):44-48.

27. Gustafsson MG. Surpassing the lateral resolution limit by a factor of two using structured illumination microscopy. *J Microsc*. 2000;198(Pt 2):82.

28. Keller PJ, Schmidt AD, Santella A, et al. Fast, high-contrast imaging of animal development with scanned light sheet-based structured-illumination microscopy. *Nat Methods*. 2010;7(8):637-642.

29. Shitara H, Kaneda H, Sato A, et al. Non-invasive visualization of sperm mitochondria behavior in transgenic mice with introduced green fluorescent protein (GFP). *FEBS Lett*. 2001;500(1-2):7-11.

30. Shim K. Vibratome sectioning for enhanced preservation of the cytoarchitecture of the mammalian organ of corti. *J Vis Exp*. 2011;(52). pii: 2793. doi(52):10.3791/2793.

31. Schindelin J, Arganda-Carreras I, Frise E, et al. Fiji: An open-source platform for biological-image analysis. *Nat Methods*. 2012;9(7):676-682.

32. Schneider CA, Rasband WS, Eliceiri KW. NIH image to ImageJ: 25 years of image analysis. *Nat Methods*. 2012;9(7):671-675.

33. Agard DA, Sedat JW. Three-dimensional architecture of a polytene nucleus. *Nature*. 1983;302(5910):676-681.

34. Otsu N. A threshold selection method from gray-level histograms. *IEEE Trans Sys , Man , Cyber*. 1979;smc-9(1):62.

35. Ridler T, Calvard S. Picture thresholding using an Iterative selection method. *IEEE Trans Pattern Anal Mach Intell*. 1978;smc-8(8):630.

36. Newman T, Yi H. A survey of the marching cubes algorithm. *Computers & Graphics*. 2006;30:854.

37. Coelho LP, Shariff A, Murphy RF. Nuclear segmentation in microscope cell images: A hand-segmented dataset and comparison of algorithms. *Proc IEEE Int Symp Biomed Imaging*. 2009;5193098:518-521.